ISSN(Online): 2319-8753
ISSN (Print): 2347-6710

International Journal of Innovative Research in Science, Engineering and Technology

(A High Impact Factor, Monthly Peer Reviewed Journal)

Vol. 5, Issue 1, January 2016

Impedance and Dielectric Studies of Lead-Cobalt Mixed Levo Tartrate Crystals

Harshkant Jethva[1*], Dinesh Kanchan[2], Mihir Joshi[1]

Associate Professor, M. M. Science College, Morbi, Gujarat, India[1*]

Professor, Department of Physics, Saurashtra University, Rajkot, Gujarat, India[1]

Professor, Department of Physics, Faculty of Science, The M S University of Baroda, Vadodara, Gujarat, India[2]

ABSTRACT: Various pure and mixed metal tartrate compounds find different applications. In the present study, the lead-cobalt mixed levo tartrate crystals with different compositions were grown by using gel growth technique. Long, dendrite, white crystals as well as reddish spherulitic crystals were grown. From EDAX the exact composition of lead and cobalt was estimated in the grown crystals. The amount of Pb was found to be much higher than Co. The powder XRD studies indicated that the unit cell parameters of Pb-Co tartrate were closer to the Pb tartrate due to higher amount of Pb in the mixed crystals. The stoichiometric formula of different composition of mixed Pb-Co tartrate was suggested. The impedance spectroscopic studies were carried out on pelletized samples from 100 Hz to 2 MHz range at room temperature. The variation of the real and imaginary part of impedance was studied with frequency of applied field. The Nyquist plot of pure Pb levo tartrate crystal exhibited the presence of two semi circles, whereas Pb-Co levo tartrate crystals showed only one semi circle. The effect of additive was clearly shown in the Nyquist plot. The variation of dielectric constant and loss with frequency was also carried out. The variation of ac conductivity with frequency has been discussed according to Jonscher's law.

KEYWORDS: Lead-cobalt mixed levo tartrate crystals, gel growth, impedance spectroscopy, dielectric study, ac conductivity, Jonscher's law.

I. INTRODUCTION

The metal tartrate compounds find various applications, for example, carbonate solutions containing Co(II) tartrate complexes in an electrochemical procedure of anodic deposition of cobalt oxihydroxide film on a glassy carbon substrate in an alkali medium [1], lead tartrate as an additive in gasoline to prevent knocking in motors [2], piezoelectric application of cadmium tartrate [3] and iron (III) tartrate acting as a photo activator in light induced oxidative degradation of white wine [4]. The growth and characterization of several metal tartrate crystals has been reported, for example, lead tartrate [5,6], iron tartrate [7], mixed iron-manganese tartrate [8], ternary iron-manganese-cobalt tartrate [9], ternary iron-manganese-nickel tartrate compound [10], mixed lead-cadmium levo tartrate [11] and mixed lead-iron levo tartrate crystals [12].
Impedance spectroscopy is very important tool to investigate the electrical properties of materials. It can be used to derive several parameters which are categorized as (a) electrolyte, such as conductivity, dielectric constant, mobility of charges, equilibrium concentration of the charged spices and bulk generation-recombination rates, etc. and (b) electrode-electrolyte interface, such as adsorbed reaction rate constants, capacitance of the interface region, diffusion coefficient of the neutral spices present in the electrode, etc. [13]. The impedance spectroscopy study has been reported for several types of compounds, for instance, nano particles [14], perovskite compounds [15], ferroelectric ceramics [16], CuO nanograins [17], polycrystalline compounds [18] and lead-iron mixed levo-tartrate crystals [19]. Earlier, several authors reported dielectric

ISSN(Online): 2319-8753
ISSN (Print): 2347-6710

International Journal of Innovative Research in Science, Engineering and Technology

(A High Impact Factor, Monthly Peer Reviewed Journal)

Vol. 5, Issue 1, January 2016

studies of metal tartrate crystals, for instance, pure metal tartrate [20], doped metal tartrates [21] and ternary metal tartrate [9] crystals. However, no major work is reported on impedance spectroscopy in metal tartrate crystals except the report on lead-iron levo tartrate crystals [19].
In the present study, the authors have grown mixed cobalt-lead levo tartrate crystals by varying composition of supernatant solution using gel growth technique and characterized mainly by impedance spectroscopy. To evaluate the composition, structure and stoichiometry the authors carried out powder XRD, EDAX, and TGA studies.

II. MATERIALS AND METHOD

In the present study, the single diffusion gel growth technique was employed to grow mixed levo tartrate crystals of cobalt and lead. The growth medium was silica hydro gel, which was set by mixing sodium metasilicate solution of specific gravity 1.05 with 1 M levo tartaric acid solution in such a manner that the pH of the mixture was obtained 4.5. This solution was poured in test tubes of 150 mm length and 25 mm diameter to set in the gel form. The following mentioned compositions of supernatant solutions were poured gently on the set gels:
(a) 1 M, 2 ml $Pb(NO_3)_2$ + 1 M, 8 ml $Co(NO_3)_2\,6H_2O$ .....(Sample A)
(b) 1 M, 4 ml $Pb(NO_3)_2$ + 1 M, 6 ml $Co(NO_3)_2\,6H_2O$ .....(Sample B)
(c) 1 M, 6 ml $Pb(NO_3)_2$ + 1 M, 4 ml $Co(NO_3)_2\,6H_2O$ .....(Sample C)
(d) 1 M, 8 ml $Pb(NO_3)_2$ + 1 M, 2 ml $Co(NO_3)_2\,6H_2O$ .....(Sample D)
All the chemicals were of AR grade and obtained from Sigma Aldrich. The following reaction was expected to occur in the formation of lead iron mixed levo tartrate crystals.

$$(X)Pb(NO_3)_2 + (1\text{-}X)Co(NO_3)_2{\cdot}6H_2O + H_2C_4H_4O_6 + nH_2O \rightarrow Pb_XCo_{(1-X)}C_4H_4O_6{\cdot}\, nH_2O + 4HNO_3 + 5H_2O + 1/2O_2$$

Where, the value of X is to be determined from the EDAX analysis exactly.
Figures 1 (a-d) are the photographs of the crystals growing inside the test tubes for the supernatant solutions (a), (b), (c), and (d), respectively.

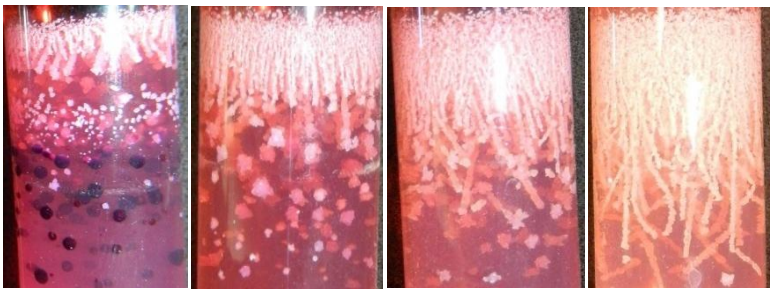

1(a) 1(b) 1(c) 1(d)

Fig. 1. Growth of crystals inside the test tube

It is observed that the crystals grown at the gel-liquid interface are dendrite in nature and white in colour. The number density and length of the dendrite crystals are changed as per the composition of the supernatant solutions. At the bottom of the test tubes, the crystals are spherulitic in nature and reddish in colour. The morphology of the crystals grown at the bottom of the test tubes is also changed as per the composition of the supernatant solutions. The dendrite type [11] and spherulite type [7] natures of the gel grown crystals have already been discussed in detail elsewhere.

ISSN(Online): 2319-8753
ISSN (Print): 2347-6710

International Journal of Innovative Research in Science, Engineering and Technology

(A High Impact Factor, Monthly Peer Reviewed Journal)

Vol. 5, Issue 1, January 2016

III. CHARACTERIZATION TECHNIQUES

The determination of metallic elements in the crystals was carried by the EDAX using Philips Xl – 30. TGA carried out from room temperature of 30^{o}C at a heating rate of 10^{o}C/min in atmosphere of air using Linseis (STA PT 1600) set up. The synthesized samples of Pb – Co levo tartrate crystals were grind to very fine powder and made into pellets without any binder. As the samples are organo-metallic compounds, they may react with the conductive layers of the coating material. Therefore, pellets without any coating were used for impedance measurements. The density and porosity of the pellets were not measured but the pellets were prepared by applying a pressure of 5 ton/sq.cm. The real and imaginary parts of complex impedance were measured using the pellets of different compositions of Pb and Co as a function of frequency ranging from 100 Hz to 2 MHz at room temperature using SI – 1260 Solartron impedance/gain phase analyzer. The obtained impedance data were analyzed by the equivalent circuit software. In this software, all the circuit parameters are adjusted simultaneously in order to fit the measured data and to obtain resistances, capacitances and circuit description code of the equivalent circuit of the sample material. The values of dielectric constant and ac conductivity were calculated by using formulations available in the literature [22].

IV. RESULT AND DISCUSSION

The composition of grown crystals was determined by EDAX. The expected and observed values of atomic weight percentage of lead and cobalt mixed crystals grown at the gel-liquid interface as well as grown below the gel-liquid interface for the samples (A)-(D) have been given by the present authors elsewhere [23]. The stoichiometric formulations are proposed on the basis of EDAX results in Table 1.

Table 1: EDAX result for Pb-Co mixed levo tartrate crystals

Sample	Expected stoichiometric formula	Obtained stoichiometric formula from EDAX results	
		Dendrite crystals at gel-liquid interface	Spherulitic crystals below gel-liquid interface
A	$Pb_{0.2}Co_{0.8}C_4H_4O_6{\cdot}nH_2O$	$Pb_{0.987}Co_{0.013}C_4H_4O_6{\cdot}nH_2O$	$Pb_{0.458}Co_{0.542}C_4H_4O_6{\cdot}nH_2O$
B	$Pb_{0.4}Co_{0.6}C_4H_4O_6{\cdot}nH_2O$	$Pb_{0.994}Co_{0.006}C_4H_4O_6{\cdot}nH_2O$	$Pb_{0.993}Co_{0.007}C_4H_4O_6{\cdot}nH_2O$
C	$Pb_{0.6}Co_{0.4}C_4H_4O_6{\cdot}nH_2O$	$Pb_{0.997}Co_{0.003}C_4H_4O_6{\cdot}nH_2O$	$Pb_{0.994}Co_{0.006}C_4H_4O_6{\cdot}nH_2O$
D	$Pb_{0.8}Co_{0.2}C_4H_4O_6{\cdot}nH_2O$	$Pb_{0.998}Co_{0.002}C_4H_4O_6{\cdot}nH_2O$	$Pb_{0.998}Co_{0.002}C_4H_4O_6{\cdot}nH_2O$

From the table 1, it is observed that the percentage weight of cobalt is very less in the dendrite crystals at the gel-liquid interface of samples (A-D) and in the spiky spherulitic crystals below the gel-liquid interface of samples (B-D), which may be due to higher hydrated radii of Co^{+2} ions compared to Pb^{+2} ions. In the solution of lead nitrate and cobalt nitrate, Pb^{+2} and Co^{+2} ions possess a primary hydration shell. Hydration of an ion depends on the electrostatic attraction of water molecules to that ion. Attraction of water molecules depends on the density of charge of ion. The smaller ions having greater ionic potential attract more water molecules. The result is the inverse relationship between non-hydrated radius and hydrated radius. In the present study, the non-hydrated radius and second ionization potential of Pb^{+2} are 1.19 Å and 15.028 eV and Co^{+2} are 0.65 Å and 17.06 eV. Therefore, the reverse nature is observed for hydrated radii of Pb^{+2} and Co^{+2} than that of non-hydrated ones [24,25]. As the hydrated radius of Co^{+2} being higher than the hydrated radius of Pb^{+2}, the Co^{+2} ions enter into the reaction in lower concentration than Pb^{+2} ions, which is resulting in lower percentage weight of cobalt in the grown crystals than lead. This has been discussed elsewhere in detail [23].

ISSN(Online): 2319-8753
ISSN (Print): 2347-6710

International Journal of Innovative Research in Science, Engineering and Technology

(A High Impact Factor, Monthly Peer Reviewed Journal)

Vol. 5, Issue 1, January 2016

It can be noticed from table 1 that, except for sample (A), in all the samples the weight percent of cobalt is well below 1% and hence only the sample (A) of spherulitic crystals grown in the bottom of gel column is characterized by different techniques along with other samples.

Powder XRD Study

The powder XRD patterns of the dendrite crystals and spherulitic crystals grown at the gel-liquid interface and below the gel-liquid interface of sample (A) is shown in the figure (2a) and (2b), respectively. Almost the similar behavior was observed for the dendrite crystals at the gel-liquid interface of samples (B-D) which has been discussed elaborately elsewhere by the present authors [23].

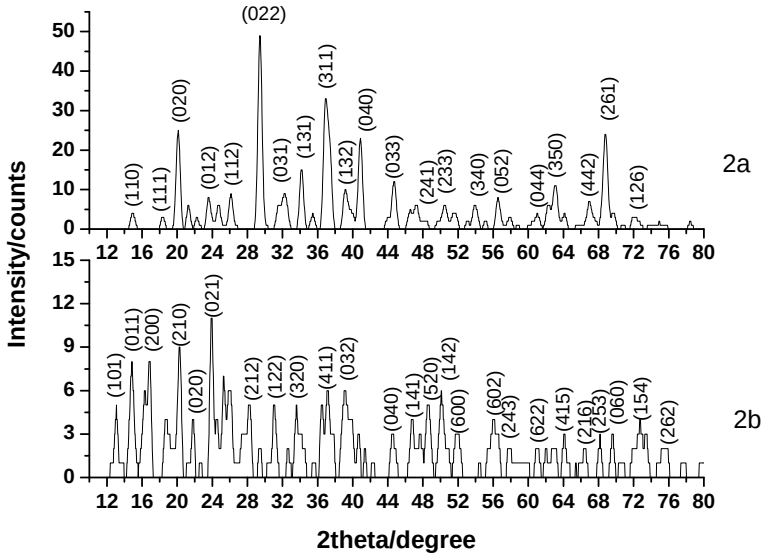

Fig. 2. Powder XRD patterns of dendrite (a) and spherulitic (b) type crystals for sample - A

The ionic radius of cobalt (0.65 Å) being low compared to lead (1.19 Å), the doping of cobalt produced no significant strain in the structure of Pb levo tartrate [26]. No separate phase due to the presence of cobalt was identified. The orthorhombic unit cell parameters of lead tartrate crystals are a = 7.99482 Å, b = 8.84525 Å and c = 8.35318 Å with space group $P2_12_12_1$ [27], while the orthorhombic unit cell parameters of cobalt tartrate crystals are a = 9.9873 Å, b = 7.8973 Å, c = 10.9832 Å with space group $P2_12_12$ [28]. In the present study, the unit cell parameters of dendrite type Pb-Co levo tartrate crystals at gel-liquid interface are: a = 7.9940 Å, b = 8.8350 Å, c = 8.3530 Å for sample (A), a = 7.9920 Å, b = 8.8380 Å, c = 8.3520 Å for sample (B), a = 7.9910 Å, b = 8.8395 Å, c = 8.3510 Å for sample (C) and a = 7.9905 Å, b = 8.8395 Å, c = 8.3510 Å for sample (D), which are found close to the unit cell parameters of pure lead tartrate. This is due to very low weight percentage presence of cobalt in the Pb-Co levo tartrate crystals. While, the unit cell parameters of spherulitic type Pb-Co levo tartrate crystals below gel-liquid interface are a = 10.58 Å, b = 8.105 Å, c = 8.90 Å for sample (A). This indicates the higher weight percentage presence of cobalt compared to lead in Pb-Co levo tartrate crystals altered its unit cell parameters and attempt to approach to the unit cell parameters of cobalt tartrate.

ISSN(Online): 2319-8753
ISSN (Print): 2347-6710

International Journal of Innovative Research in Science, Engineering and Technology

(A High Impact Factor, Monthly Peer Reviewed Journal)

Vol. 5, Issue 1, January 2016

Thermal Study

The TG curves of the dendrite crystals and spherulitic crystals grown at the gel-liquid interface and below the gel-liquid interface of sample (A) is shown in the figure (3a) and (3b), respectively. Almost the similar behavior is observed for the dendrite crystals at the gel-liquid interface of samples (B-D) [23].

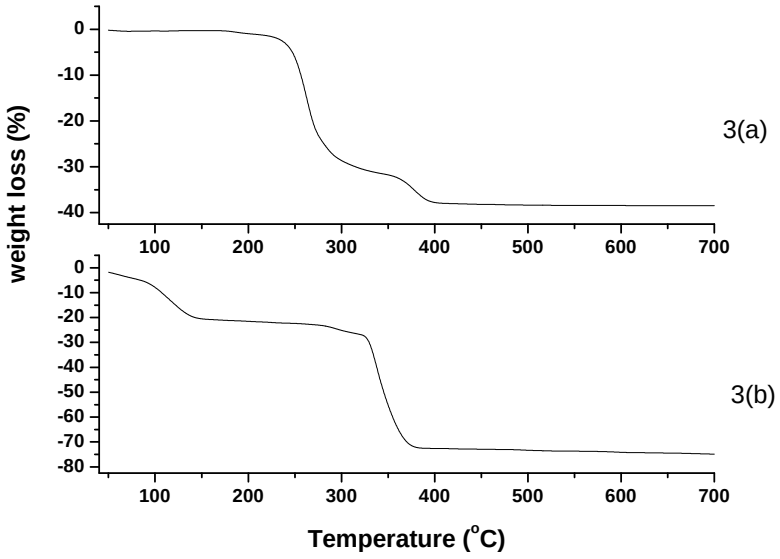

Fig. 3. TG traces for dendrite (a) and spherulite (b) crystals of sample – A

The samples (A-D) are converted into anhydrous form within 250°C. The anhydrous form of samples (A-C) and sample (D) is converted into carbonate form and oxalate form at temperature of 280°C and 300°C, respectively. Finally, the carbonate form of samples (A-C) is converted into oxide form at 400°C, while oxalate form of sample (D) is converted into carbonate form at 380°C and further converted into oxide form at 440°C. For the spherulitic crystals of sample (A), no decomposition is observed upto 50°C. Between 50 to 150°C, the sample is converted into anhydrous form. The anhydrous form remains almost stable upto 340°C and then the sample is converted into oxide form at temperature 380°C. The detailed analysis is discussed by the present authors elsewhere [23]. The amount of water molecules attached with the dendrite crystals of samples (A-D) and spherulitic crystals of sample (A) have been calculated and given in table 2 with stoichiometric formula.

Table 2. Stoichiometric formula for Pb-Co mixed levo tartrate crystals

Sample name	Estimated formula from EDAX and TGA
Dendrite crystals of sample (A)	$Pb_{0.987}Co_{0.013}C_4H_4O_6{\cdot}0.15H_2O$
Dendrite crystals of sample (B)	$Pb_{0.994}Co_{0.006}C_4H_4O_6{\cdot}0.2H_2O$
Dendrite crystals of sample (C)	$Pb_{0.997}Co_{0.003}C_4H_4O_6{\cdot}0.2H_2O$
Dendrite crystals of sample (D)	$Pb_{0.998}Co_{0.002}C_4H_4O_6{\cdot}0.2H_2O$
Spherulitic crystals of sample (A)	$Pb_{0.458}Co_{0.542}C_4H_4O_6{\cdot}6H_2O$

ISSN(Online): 2319-8753
ISSN (Print): 2347-6710

International Journal of Innovative Research in Science, Engineering and Technology

(A High Impact Factor, Monthly Peer Reviewed Journal)

Vol. 5, Issue 1, January 2016

Impedance Study

Generally, the data in the complex plane could be represented in any one of the four basic forms such as complex impedance (Z^*), complex admittance (Y^*), complex permittivity (ε_r^*) and complex modulus (M^*). The complex impedance representation is used when the relaxation times of various processes differ as a consequence of different capacitive components. The complex impedance plot, called the Nyquist plot, gives one or two semi-circular arcs, depending upon the relative values of their relaxation times. Each of these semicircles could be represented by a single RC combination. The semicircle passes through a maximum at a frequency f_r, called the relaxation frequency and satisfies the condition $\omega\tau = 1$. On the other hand, complex modulus or permittivity plane plots are used to represent the response of dielectric systems [29]. Complex impedance plane plots of Z' versus Z'' are useful for determining the dominant resistance of a sample but are insensitive to the smaller values of resistances, while the complex modulus plots are useful in determining the smallest capacitance. Sinclair and West [30] suggested the combined usage of impedance and modulus spectroscopic plots to rationalize the dielectric properties. Characterization of various electro-materials [31], thin films [32], Co-implanted ZnO single crystals [33], CuO nano-grains [17] and Pb-Fe mixed levo-tartrate crystals [19] have been reported in terms of equivalent circuits and their circuit components contributions.

Figure (4a) and figure (5a) show the Nyquist diagram (Z'' vs. Z') at room temperature for pure Pb levo-tartrate crystals and dendrite crystals of Pb-Co levo tartrate grown at the gel-liquid interface of samples (A-D) and spherulitic crystals grown below the gel-liquid interface of sample (A).

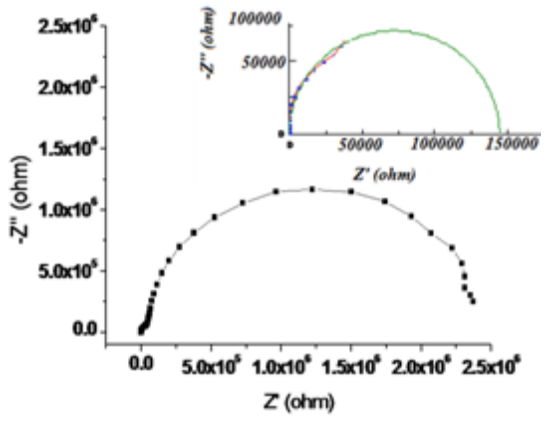

Fig. 4a. Nyquist plot Pure Pb levo tartrate crystals

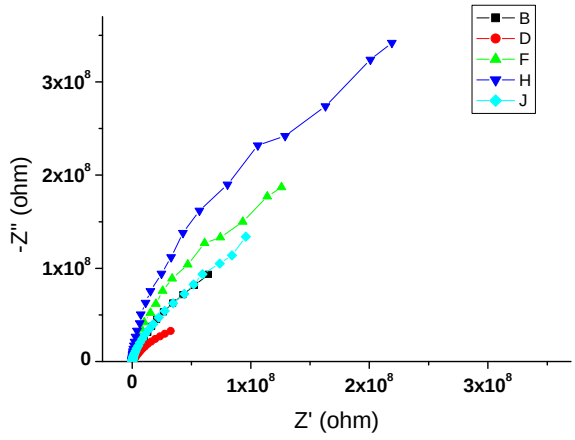

Fig. 5a. Nyquist plot Pb-Co levo tartrate crystals

In the figure (5a), B, D, F and H represent Nyquist plots for dendrite crystals of samples (A-D) and (J) for spherulitic crystals of sample (A).

The best fit equivalent model circuit was obtained by using the software Z-view. The value of grain resistance (R_g) and corresponding grain capacitance (C_g) as well as grain-boundary resistance (R_{gb}) and corresponding grain-boundary capacitance (C_{gb}) and corresponding relaxation frequency were obtained by using software Z-view under simulation of data to obtain the best fit equivalent circuit.

A closer look at the Nyquist plot for the pure lead levo-tartrate crystals of figure (4a) clearly indicates the steep rising arc and a presence of a one more semi-circle near the origin. The inset figure 4(a) indicates the presence of semi circle arc after fitting data with software Z view in the high frequency region near the origin. This is represented in the form of two parallel

ISSN(Online): 2319-8753
ISSN (Print): 2347-6710

International Journal of Innovative Research in Science, Engineering and Technology

(A High Impact Factor, Monthly Peer Reviewed Journal)

Vol. 5, Issue 1, January 2016

RC elements in series as shown in figure (4b). The two semi-circular arcs in the impedance plane plots show the presence of two relaxation process in the system with different relaxation frequencies. The low and high frequency arcs are attributed to the relaxation of the charge carriers at grain boundaries and grain interiors, respectively.

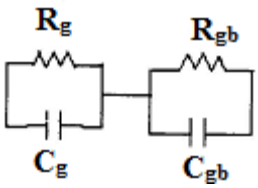

Fig. 4b. Equivalent circuit Pure Pb levo tartrate crystals

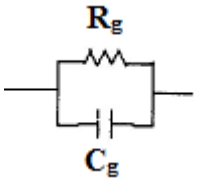

Fig.5b. Equivalent circuit Pb-Co levo tartrate crystals

As the cobalt content is added into the pure Pb levo-tartrate sample, the high frequency semi-circular arc is disappeared and only the initial part of the arc for all the five samples of Pb-Co levo-tartrate crystals exist, which is shown in the Nyquist plot of figure (5a). Polycrystalline materials are heterogeneous in nature due to effects of grains and grain boundaries in the ac electrical properties [18]. Due to less thickness of grain boundaries compared to grain interiors, grain boundaries offer high resistance. Therefore, larger is the product RC and lower would be the relaxation frequency. A parallel RC combination (R_g, C_g), shown in figure (5b), is found to have excellent fit with the experimental data, there by indicating the contribution from grains of the samples. The centers of all the three semicircles lie below the real axis having comparatively large radii. There is no systematic change observed in the radii of semi circles for the dendrite crystals of samples (A-D) with the composition of the samples indicating no systematic variation in the resistivity of the samples with the composition of the samples. This may be due to very low weight percentage (1.3% and less) presence of cobalt in the samples.

The values of R_g, R_{gb}, C_g, C_{gb} and relaxation frequency for the pure Pb levo-tartrate crystals and the values of R_g, C_g and relaxation frequency for the Pb-Co levo-tartrate crystals at room temperature are obtained by using the software Z view and listed in table 3.

With comparison to pure lead levo tartrate crystals the values of grain resistances are high in Pb-Co levo tartrate crystals and indicate the clear effect of presence of additive. In the Nyquist curve of pure lead levo tartrate, the equivalent circuit shows the effect of both grain and grain boundaries, while in the lead-cobalt levo tartrate the equivalent circuit shows the effect of increasing grain resistances and absence of grain boundary resistances. It is found that the majority amount of cobalt enters the crystalline lattice due to substitutional nature of cobalt and the grain resistance changes. There is a marked change in the electrical properties and equivalent circuits found in pure lead levo tartrate on addition of cobalt. It is observed from the table 3 that there is no systematic variation in the values of grain resistances for Pb-Co levo tartrate crystals, which may be due to the combine role of water of hydration/moisture and very low percentage weight of cobalt in the sample., i.e., around 1% atomic weight percentage.

ISSN(Online): 2319-8753
ISSN (Print): 2347-6710

International Journal of Innovative Research in Science, Engineering and Technology

(A High Impact Factor, Monthly Peer Reviewed Journal)

Vol. 5, Issue 1, January 2016

Table 3: Grain and grain boundary resistances and capacitances

Sample Name	R_g (MΩ)	R_{gb} (MΩ)	C_g (pF)	C_{gb} (pF)	Relaxation frequency
$PbC_4H_4O_6$ $2.4H_2O$	0.145	2.38	103	66.5	f_g = 10.6 kHz f_{gb} = 1 kHz
Dendrite crystals sample (A) $Pb_{0.987}Co_{0.013}C_4H_4O_6{\cdot}0.15H_2O$	359	--------	50.4	--------	f_g = 10 Hz
Dendrite crystals sample (B) $Pb_{0.994}Co_{0.006}C_4H_4O_6{\cdot}0.2H_2O$	118	--------	55.9	--------	f_g = 22 Hz
Dendrite crystals sample (C) $Pb_{0.997}Co_{0.003}C_4H_4O_6{\cdot}0.2H_2O$	535	--------	21.7	--------	f_g =15 Hz
Dendrite crystals sample (D) $Pb_{0.998}Co_{0.002}C_4H_4O_6{\cdot}0.2H_2O$	750	--------	6.88	--------	f_g = 30 Hz
Spherulitic crystals sample (A) $Pb_{0.458}Co_{0.542}C_4H_4O_6{\cdot}6H_2O$	351	--------	17.1	--------	f_g = 25 Hz

Dielectric Study

The real part of dielectric constant (ε') and imaginary part of dielectric constant (ε'') are calculated from impedance values by using the following formulations:

$$\varepsilon' = \frac{t}{\omega A \varepsilon_0}\frac{Z''}{Z'^2+Z''^2} = \frac{t}{2\pi f A \varepsilon_0}\frac{Z''}{Z^2} \quad .....(1) \qquad \varepsilon' = \frac{t}{2\pi f A \varepsilon_0}\frac{Z'}{Z^2} \quad .....(2)$$

Where, A = Cross-section area of the pellet, t = Thickness of the pellet, ε_0 = Permittivity of free space = 8.854×10^{-12} F/m and $Z^2 = Z'^2 + Z''^2$.

Figure 6 shows the variation of real part of dielectric constant (ε') with frequency and figure 7 shows the variation of dielectric loss with frequency.

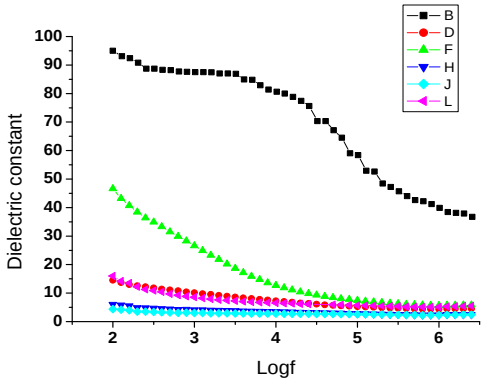

Fig. 6. Plots of dielectric constant versus frequency (B) for pure lead levo tartrate crystals, (D, F, H, J) for dendrite crystals of Pb-Co levo tartrate of samples (A-D) and L for spherulitic crystals of Pb-Co levo tartrate of sample (A)

ISSN(Online): 2319-8753
ISSN (Print): 2347-6710

International Journal of Innovative Research in Science, Engineering and Technology

(A High Impact Factor, Monthly Peer Reviewed Journal)

Vol. 5, Issue 1, January 2016

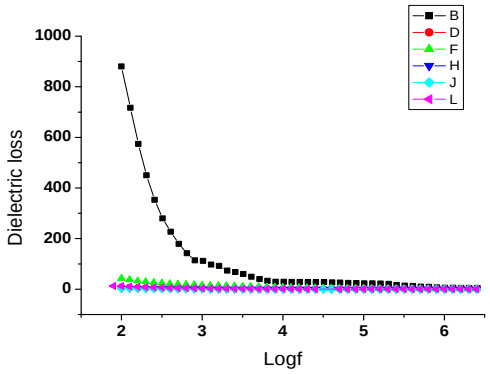

Fig. 7. Plots of dielectric loss versus frequency (B) for pure lead levo tartrate crystals, (D, F, H, J) for dendrite crystals of Pb-Co levo tartrate of samples (A-D) and L for spherulitic crystals of Pb-Co levo tartrate of sample (A)

It is seen that the values of both dielectric constant and dielectric loss decrease with increase in frequency, which is a common feature in many compounds such as iron-nickel-manganese ternary levo-tartrate crystals [10], lead-iron mixed levo-tartrate crystals [19], zinc tartrate [20], 4-(2-hydroxyphenylamino)-pent-3en-2-one (HPAP) [34], and zinc doped nano-hydroxyapatite [35]. The high value of dielectric constant at lower frequencies may be due to the presence of all the four types of polarizations, viz., electronic, ionic, orientation and space charge are prominent in the low frequency region and its low value at higher frequencies may be due to the loss of significance of some of these polarizations gradually. At low frequencies, the dipoles can easily switch the alignment with the changing field. As the frequency increases, both the dielectric constant and dielectric loss values are found to decrease and attain lower values which indicate that the dipoles do not comply with oscillating electric field and maintain their phase, thus they reduce their contribution to the polarization. The low power dissipation in the crystals is indicated by low dielectric loss values at higher frequencies. In the dielectric measurements as the capacitance of the sample is proportional to the dielectric constant, the addition of cobalt reduces the grain capacitance of Pb levo tartarte, which further results in the reduction of dielectric constant of the Pb-Co levo tartrate crystals. With comparison to pure lead levo tartrate crystals the dielectric loss is very low in lead-cobalt levo tartrate crystals is due to the presence of cobalt at grain position reducing the grain capacitance and ultimately the dielectric loss. The non-systematic variation in the dielectric constant of Pb-Co levo tartrate as shown in the figure 6 with composition of Co in the crystals may be due to the combine role of water of hydration and composition of the crystals.

AC Conductivity Analysis

When the conductivity is measured with an ac frequency $\omega = 2\pi\upsilon$, the response of the material, either crystalline or amorphous, can be represented by an equation proposed by Jonscher [36].

$\sigma_{total} = \sigma_{dc} + \sigma_{ac}(\omega) = \sigma_{dc} + A\omega^n$ .....(3)

where, σ_{dc} is the direct current or static conductivity due to excitation of electron from a localized state to the conduction band, $A\omega^n$ is the ac conductivity due to the dispersion phenomena occurring in the material. A is a temperature dependent constant which determines the strength of polarizibility [37] and n is a function of temperature as well as frequency, which generally varies between 0 and 1 and represents the degree of interaction between mobile ions with the lattice around them.

ISSN(Online): 2319-8753
ISSN (Print): 2347-6710

International Journal of Innovative Research in Science, Engineering and Technology

(A High Impact Factor, Monthly Peer Reviewed Journal)

Vol. 5, Issue 1, January 2016

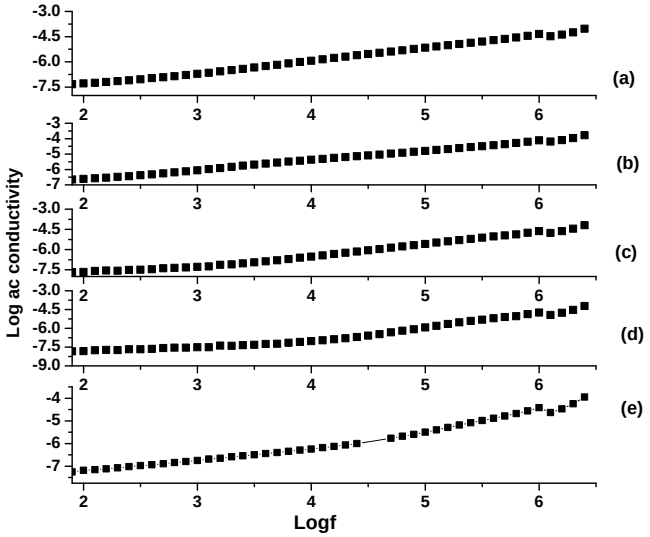

Fig. 8. Jonscher's plot (a-d) for dendrite crystals of samples (A-D) and (e) for spherulite crystals of sample (A)

In the figure 8, (a-d) the Jonscher's Plots for the dendrite crystals of samples (A-D) and (e) for the spherulitic crystals of sample (A) are shown. It is clear from the plots that the conductivity remains constant for all the samples in the low frequency region. Therefore, the relation $\sigma(\omega,T)\ \alpha\ \sigma_{dc}(T)$ holds well for all the samples in the low frequency region. Thereafter, as the frequency increases, the ac conductivity also increases and hence, the relation $\sigma(\omega,T)\ \alpha\ \omega^n$ holds well for all the samples. A plot of ac conductivity versus angular frequency on logarithmic scale yields the value of exponent *n* and constant *A*, which are listed in table 4.

Table 4: The values of *n*, *A* and σ_{dc} for the pure Pb levo-tartrate crystals and mixed Pb-Co levo-tartrate crystals

Sample	*n*	$A \times 10^{-10}$ (S m^{-1} rad^{-n})	$\sigma_{dc} \times 10^{-8}$ (S m^{-1}) (from formula)	$\sigma_{dc} \times 10^{-8}$ (S m^{-1}) (from plot)
$PbC_4H_4O_6\ 2.4H_2O$	0.62	438	509	504
Dendrite crystals sample (a) $Pb_{0.987}Co_{0.013}C_4H_4O_6{\cdot}0.15H_2O$	0.74	1.3	4.94	4.64
Dendrite crystals sample (b) $Pb_{0.994}Co_{0.006}C_4H_4O_6{\cdot}0.2H_2O$	0.62	1.25	2.0	2.19
Dendrite crystals sample (c) $Pb_{0.997}Co_{0.003}C_4H_4O_6{\cdot}0.2H_2O$	0.79	2.90	1.70	2.00
Dendrite crystals sample (d) $Pb_{0.998}Co_{0.002}C_4H_4O_6{\cdot}0.2H_2O$	0.79	1.41	1.24	1.44
Spherulitic crystals sample (a) $Pb_{0.458}Co_{0.542}C_4H_4O_6{\cdot}6H_2O$	0.68	16	5.12	5.52

ISSN(Online): 2319-8753
ISSN (Print): 2347-6710

International Journal of Innovative Research in Science, Engineering and Technology

(A High Impact Factor, Monthly Peer Reviewed Journal)

Vol. 5, Issue 1, January 2016

The dc conductivity σ_{dc} for all the samples has been calculated using the relation:

$$\sigma_{dc} = \frac{t}{R_b A} \quad \text{.....(4)}$$

where t is the thickness of the pellet, A is the cross-section area of the pellet and R_b is the grain (bulk) resistance of the sample. It is found that the dc conductivity values calculated by using the formula and obtained from the Jonscher's plot are the same and listed in table 4.

It is observed from the table 4 that the value of constant *A(T)* does not vary appreciably for the dendrite crystals of samples (A-D). It means that the strength of polarizability is almost the same for the dendrite crystals of samples (A-D). This indicates that the dipoles per unit volume in all the samples can align in nearly the same manner in the direction of applied varying electric field. It is observed that there is no conclusive or significant effect of different composition of cobalt in the dendrite crystals of Pb-Co levo-tartrate on the strength of polarizability. The value of constant *A(T)* is high for the spherulitic crystals of sample (A), which indicates that the strength of polarizability is high for this crystals. This may be due to the highest percentage weight of cobalt. The variation in the value of exponent *n* is not systematic and within 0.62 to 0.79 for Pb-Co levo-tartrate crystals, indicating the degree of interaction of mobile ions with the lattice is almost the same for all the samples without significant effect of different composition of Pb and Co. All the samples are observed to obey the Jonscher's law.

The polarizability of an atom or molecule depends on its dimension. As per the simple estimate for spherical atom or molecule the polarizability is proportional to the cube of its radius [38]. The higher value of ionic radius of Pb (1.19Å) compared to Co (0.65 Å) leads higher polarizability of lead than cobalt. As per the equation $\alpha = \varepsilon_o(K - 1) / n$, where α = strength of polarizability, K = dielectric constant and n = number density, higher value of dielectric constant gives the higher value of the polarizability. The high value of polarizability of lead confirms the higher value of dielectric constant of pure Pb levo tartrate crystals than Pb-Co levo tartrate crystals. As cobalt is added into the pure Pb levo tartrate crystals, the value of A in Jonscher's equation is reduced, indicating low polarizability and dielectric constant [39]. This is in correspondence to the impedance spectroscopy study results.

Funke [40] explained the physical significance of *n* in Jonscher's equation in two different regimes, i.e., $n \leq 1$ indicating that the hopping motion involved is a translational motion with a sudden hopping and $n > 1$ suggesting that the motion involved is a localized hopping of the species with a small hopping without leaving the neighborhood [41]. For ionic conductors, the value of *n* can lie between 1 and 0.5 indicating the ideal long range pathways and diffusion limited hopping (tortuous pathways) [42]. The Jump Relaxation Model (JRM) developed by Funke and Riess [43] attributes the dispersion in the conductivity to strong forward-backward jump correlations in the motion of ions.

The variation of dielectric constant with frequency of applied field is within the values of 93 to 34 for pure Pb levo-tartrate crystals, 14.5 to 4.5 for dendrite crystals of sample (A), 46.5 to 5.8 for dendrite crystals of sample (B), 6.1 to 2.45 for dendrite crystals of sample (C), 4.36 to 2.44 for dendrite crystals of sample (D) and 16 to 5.46 for spherulitic crystals of sample (A). This variation is measured within the frequency range 80 Hz to 2.5 MHz. According to the classification proposed by Singh and Ulrich [44] the high dielectric materials have $K > 7$ and the low dielectric materials have $3.9 > K$. Comparing the dielectric results with this classification, the present samples possess high values of dielectric constant and they may find the application mainly in three areas such as memory cell dielectrics, gate dielectrics and passive components [44] after complete electrical and physical characterizations.

V. CONCLUSIONS

The lead-cobalt levo-tartrate crystals of different composition were grown in silica gel with varying the mixture of lead nitrate and cobalt nitrate in supernatant solutions. The correct stoichiometric formulae of Co-Pb levo tartrate crystals

ISSN(Online): 2319-8753
ISSN (Print): 2347-6710

International Journal of Innovative Research in Science, Engineering and Technology

(A High Impact Factor, Monthly Peer Reviewed Journal)

Vol. 5, Issue 1, January 2016

obtained from EDAX and TGA corresponded the earlier reported work by the present authors. The Nyquiest diagram of lead levo tartrate was composed of two semi circles, which indicated the presence of grain and grain boundary effect; but for the Pb-Co levo tartrate crystals only one semi circle was exhibited indicating the effect of grain only. The dielectric constant and dielectric loss both decreased with increasing frequency. The dielectric constant changed very less and in non-systematic manner with the different composition of the samples for Pb-Co levo tartrate crystals, which may be due to the combine role of water of hydration/moisture and composition of the samples. The values of dielectric constants were comparatively less for Pb-Co levo tartrate crystals than pure Pb levo tartrate crystals, which was due to the presence of cobalt having less polarizability than lead. The conductivity variation with frequency was found to fit with the Jonscher's power law expression. The effect of presence of cobalt was exhibited very well in the conductivity values with comparison to the pristine lead levo tartrate crystals. The value of n indicated the motion involved of charge carriers is a translational motion with sudden hopping. The effect of cobalt content in the samples was found to be negligible in Pb-Co levo tartrate crystals as the content variation was below 1.07%, however the impedance spectroscopy and dielectric study was found to be very sensitive to dopant presence with respect to the pure samples.

ACKNOWLEDGMENTS

The authors are thankful to the HOD Physics (Saurashtra University, Rajkot and M. S. University, Vadodara) for their kind co-operation. The author (HOJ) is thankful to the Principal and Management of Maharaja Shree Mahendrasinhji Science College, Morbi, Gujarat, India for the encouragement. The authors acknowledge the financial assistance under SAP DRS-II and DST FIST.

REFERENCES

[1] I.G. Casella, Electrodeposition of cobalt oxide films from carbonate solutions containing Co(II) tartrate complexes, J. Electroanal. Chem. 520(1-2) (2002) 119-125.
[2] N.J. Rahway, The Merck Index of Chemicals and Drugs. 6thedn. Merck & Co. (1952)
[3] J.S. Hopwood, A.W. Nicol, Crystal data of cadmium tartrate pentahydrate. Crystallogr. J. Online 1600 (1972) 5767.
[4] A.C. Clark, D.A. Dias, T.A. Smith, K.P. Ghiggino, G.R. Scollary, Iron(III) Tartrate as a Potential Precursor of Light-Induced Oxidative Degradation of White Wine: Studies in a Model Wine System. J. Agric. Food Chem. 59(8) (2011) 3575-3581.
[5] M. Abdulkadhar, M.A. Ittyachen, Development of lead tartrate crystals from its dendritic form. J. Cryst. Growth 39 (1977) 365.
[6] H.O. Jethva, M.V. Parsania, Growth and characterization of lead tartrate crystals. Asian J. Chem. 22(8) (2010) 6317.
[7] S. Joseph, H.S. Joshi, M.J. Joshi, Infrared spectroscopic and thermal studies of gel grown spherulitic crystals of iron tartrate. Cryst. Res. Technol. 32(2) (1997) 339-346.
[8] S.J. Joshi, B.B. Parekh, K.D. Parikh, K.D. Vora, M.J. Joshi, Growth and characterization of gel grown pure and mixed iron-manganese levo-tartrate crystals. Bull. Mater. Sci. 29(3) (2006) 307-312.
[9] S.J. Joshi, K.P. Tank, B.B. Parekh, M.J. Joshi, Characterization of gel grown iron-manganese-cobalt ternary levo-tartrate crystals. Cryst. Res. Technol. 45 (2010) 303-310.
[10] S.J. Joshi, K.P. Tank, B.B. Parekh, M.J. Joshi, FTIR and thermal studies of iron-nickel-manganese ternary levo-tartrate crystals. J. Therm. Anal. Calorim. doi:10.1007/s10973-012-2624-8 (2012).
[11] H.O. Jethva, P.M. Vyas, K.P. Tank, M.J. Joshi, FTIR and thermal studies of gel-grown, lead-cadmium mixed levo tartrate crystals. J. Therm. Anal. Calorim. doi:10.1007/s10973-014-3770-y (2014).
[12] H.O. Jethva, M.J. Joshi, FTIR and thermal studies of gel-grown, lead-iron-mixed levo tartrate crystals. IJEIT 4(1) (2014) 121-127.
[13] J, Ross Macdonald, Impedance Spectroscopy, John Wiley, New York (1987).
[14] R. Triphathi, A. Kumar, T.P. Sinha, Dielectric properties of CdS nanoparticles synthesized by soft chemical route. Pramana J. Phys. 72(6) (2009) 969-978.
[15] M.P. Dasari, K. Sambasiva Rao, P. Murali Krishna, G. Gopala Krishna, Barium strontium bismuth niobate layered perovskites: Dielectric, impedance and electrical modulus characteristics. Acta Physica Polonica A 119 (2011) 387-394.
[16] P. Ganguly, A.K. Jha, Structural, dielectric and electrical properties of $CaBa_4SmTi_3Nb_7O_{30}$ ferroelectric ceramic. Bull. Mater. Sci. 34(4) (2011) 907-914.
[17] M. Younas, M. Nadeem, M. Idrees, M.J. Akhtar, Jahn-Teller assisted polaronic hole hopping as a charge transport mechanism in CuO nanograins. Appl. Phys. Lett. 100 (2012) 152103 (1-4).

ISSN(Online): 2319-8753
ISSN (Print): 2347-6710

International Journal of Innovative Research in Science, Engineering and Technology

(A High Impact Factor, Monthly Peer Reviewed Journal)

Vol. 5, Issue 1, January 2016

[18] M. Shah, M. Nadeem, M. Idress, M. Atif, M.J. Akhtar, Change of conduction mechanism in the impedance of grain boundaries in $Pr_{0.4}Ca_{0.6}MnO_3$. J. Magn. Magn. Mater. 332 (2013) 61-66.
[19] H.O. Jethva, M.J. Joshi, D.K. Kanchan, Impedance and dielectric studies of lead-iron mixed levo-tartrate crystals. IJEIT 5(3) (2015) 99-106.
[20] R.M. Dabhi, B.B. Parekh, M.J. Joshi, Dielectric studies of gel grown zinc tartrate crystals. Indian J. Phys. 79(5) (2005) 503.
[21] S.R. Suthar, S.J. Joshi, B.B. Parekh, M.J. Joshi, Dielectric study of Cu^{+2} doped calcium tartrate tetrahydrate crystals. Indian J. Pure & appl. Phys. 45 (2007) 48-51.
[22] D.K. Pradhan, R.N.P. Choudhary, B.K. Samantaray, Studies of dielectric relaxation and ac conductivity behaviour of plasticized polymer nanocomposite electrolytes. Int. J. Electrochem. Sci. 3 (2008) 597-608.
[23] H.O. Jethva, M.J. Joshi, FTIR and thermal study of gel grown lead cobalt mixed levo-tartrate crystals. IJIRSET 3(9) (2014) 16517.
[24] Dove, Nix, Ionic hydration in chemistry and biophysics. Geochim Cosmochim Acta 61 (1997) 3331.
[25] C.F. Albert, G. Wilkinson, P.L. Gaus, Basic inorganic chemistry. 3rd ed., Wiley, p. 292 (1995).
[26] B.D. Cullity, Elements of x-ray diffraction. Addison-Wesley, p. 447 (1978).
[27] D.J.A. De Ridder, K. Goubitz, E.J. Sonneveld, W. Molleman, H. Schenk, Lead tartrate from x-ray powder diffraction data. Cryst Struct Commun C58 (2002) m596-m598.
[28] V. Mathivanan, M. Haris, T. Prasanyaa, M. Amgalan, Synthesis and characterization of gel grown cobalt tartrate crystals, Pramana J. Phys. 82(3) (2014) 537-548.
[29] S.P.S. Badwal, Proceedings of the International seminar on Solid State Ionic Devices. Singapore 165 (1988).
[30] D.C. Sinclair, A.R. West, Impedance and modulus spectroscopy of semiconducting $BaTiO_3$ showing positive temperature coefficient of resistance. J. Appl. Phys. 66(8) (1989) 3850.
[31] D.C. Sinclair, Characterization of electro-materials using ac impedance spectroscopy. Boi. Soc. Esp. Ceram. Vidrio. 34(2) (1995) 55-65.
[32] J.L. Hertz, A. Bieberle, H.L. Tuller, Characterization of the electrochemical performance of YSZ thin films with nanometer-sized grain structure. MIT-Tohoku "21 COE" Joint workshop on nano-science in energy technology. O-11-1 (2004).
[33] M. Younas et al, Impedance analysis of secondary phases in a Co-implanted ZnO single crystal. Phys. Chem. Chem. Phys. 16 (2014) 16030-16038.
[34] B.B. Parekh, D.H. Purohit, P. Sagayaraj, H.S. Joshi, M.J. Joshi, Growth and characterization of 4-(2-hydroxyphenylamino)-pent-3-en-2-onesingle crystals. Cryst Res Technol 42 (2007) 407.
[35] K.P. Tank, P. Sharma, D.K. Kanchan, M.J. Joshi, FTIR, powder XRD, TEM and dielectric studies of pure and zinc doped nano-hydroxyapatite Cryst. Res. Technol. 46 (2011) 1309.
[36] A.K. Jonscher, Dielectric Relaxation in Solids. Chelsea Dielectric Press, London (1983).
[37] C. Karthik, K.B.R. Varma, Dielectric and ac conductivity behaviour of $BaBi_2Nb_2O_9$ ceramics. J. Phys. Chem. Solids 67 (2006) 2437.
[38] R. Murugeshan, Electricity and magnetism, 7th ed., S. Chand, New Delhi (2008) p. 300.
[39] D. Shamiryan, T. Abell, F. Iacopi, K. Maex, Low k dielectric materials, Materials today, 7(1) (2004) 34-39.
[40] K. Funke, Jump relaxation in solid electrolytes, Prog. Solid State Chem., 22(2) (1993) 111-195.
[41] S. Sen, R.N.P. Choudhary, Impedance studies of Sr modified BaZr0.05Ti0.95O3 ceramics, Mater. Chem. Phys., 87(2) (2004) 256-263.
[42] K.A. Mauritz, Dielectric relaxation studies of ion motions in electrolyte containing perfluorosulfonate ionomers . 4. Long –range ion transport, Macromolecules. 22 (1989) 4483-4488.
[43] K. Funke, I. Riess, Z. Phys. Chem. Neue Folge. 140 (1984) 217.
[44] R. Singh, R.K. Ulrich, High and low dielectric constant materials, 4th Symposium, The Electrochemical Society Interface, Summer (1999) 26.